

Controlled single electron transfer between Si:P quantum dots

T. M. Buehler, V. Chan, A. J. Ferguson, A. S. Dzurak,

F. E. Hudson, D. J. Reilly*, A. R. Hamilton and R. G. Clark

Centre for Quantum Computer Technology Schools of Physics and Electrical Engineering,
University of New South Wales, NSW 2052, Australia

D. N. Jamieson, C. Yang, C. I. Pakes and S. Prawer

Centre for Quantum Computer Technology School of Physics, University of Melbourne, VIC 3010, Australia

Here we present an experimental demonstration of gate-controlled transfer of single electrons between two buried Si:P quantum dots, each containing ~ 600 phosphorus atoms, with non-invasive detection using rf single electron transistors. These results open the way to a new class of precision-doped quantum dots in silicon including the Kane Si:P quantum computer scheme which requires the ability to readout a single spin or charge. Combined with a novel single ion implantation process that enables dots to be configured with just one P atom, a path is provided towards physical realization of Si:P qubits.

Of the solid-state quantum computing (QC) [1] schemes, superconducting qubits are presently the most advanced, with demonstration of coherent control [2] and quantum logic involving two qubits [3]. Semiconductor schemes are less advanced, although a GaAs charge-based qubit has been demonstrated in a GaAs double quantum dot (QD) [4] system and recent experiments [5], [6] on single GaAs QDs indicate that coherent control of a single electron spin may be close. In Kane's original scheme [7] the qubits were defined by nuclear spin states of ^{31}P dopants in Si. Since then, other Si:P schemes have been proposed based on both spin [8], [9], [10], [11] and charge [12].

To assess the feasibility of Si:P qubits we have constructed a novel double quantum dot structure in silicon using phosphorus ion implantation, configured with surface control gates and rf-single electron transistor (rf-SET) readout circuitry (Fig. 1a). These many-electron dots have a metallic density of states separated by a barrier, enabling periodic sequential tunneling between dots upon application of a differential bias to the surface

gates. The two SETs provide non-invasive detection of this charge motion. The ability to control and detect, on rapid timescales, the motion of a single electron between these Si:P buried atom dots addresses a number of formidable challenges associated with Si:P qubits.

To construct the Si:P dots we use electron-beam lithography (EBL) to pattern nano-apertures in a polymethylmethacrylate (PMMA) ion-stopping resist, laterally defining the doped regions (Fig. 1b). We have fabricated apertures as small as 15nm, but for this study use a 30nm diameter. A 14 keV ^{31}P ion beam implants the 600 dopants per hole through a 5nm SiO_2 barrier layer to a mean depth of 20nm into the substrate [13]. Damage created during implantation is removed via a rapid thermal anneal to 1000°C for 5 seconds, sufficient to activate the P donors [14] but limiting their diffusion to $\sim 1\text{nm}$ based on bulk rates [15]. The remaining nanocircuitry on the surface is completed using two further EBL steps, aligned to the buried P dots using Ti/Pt registration markers deposited prior to implantation. The Ti/Au control gates (widths 12-30nm) are deposited first using EBL patterning of a single PMMA layer, followed by the two Al/ Al_2O_3 SETs, fabricated using a bilayer resist and double-angle metallization process [16].

To control the transfer of electrons in the double quantum dot (DQD) structures the symmetry of the double well potential is adjusted by applying a differential voltage to gates S_L and S_R . The resulting charge distribution in the DQD is then determined by monitoring the source-drain current I_{SD} of either of the two SET charge detectors on the device. In our devices, each is capacitively coupled to its target buried quantum dot using an antenna electrode 500nm long, which forms part of the SET island (see Fig. 1a).

Fig. 2a plots the SET current as V_{SL} is swept over a 100mV range for a DQD with a dot separation $d=100\text{nm}$. Throughout these measurements, compensation voltages on additional gates keep the SETs at operating points

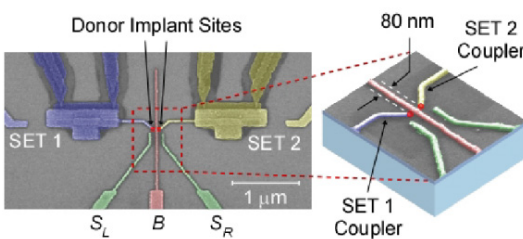


FIG. 1: SEM image of a Si:P DQD device. Three control gates S_L , B and S_R control charge transfer between the buried dots, shown schematically by red circles.

*Now at Dept. Physics, Harvard University, Cambridge MA 02138, USA

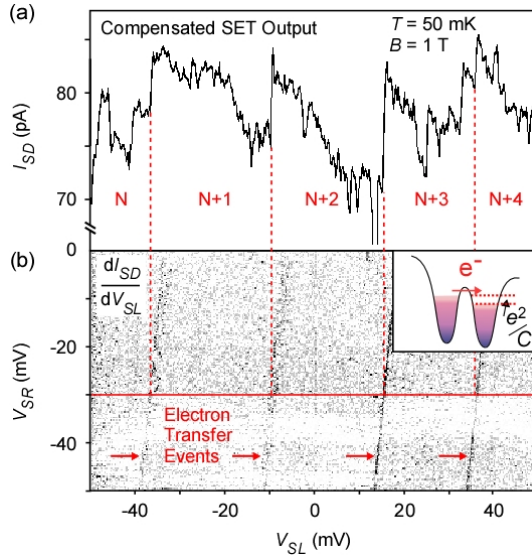


FIG. 2: Gate-controlled single electron transfer in a DQD. **a)** SET current I_{SD} as a function of V_{SL} with $V_{SR} = -30\text{ mV}$ (red line in **b**) for a DQD device with $d = 100\text{ nm}$. **b)** SET transconductance dI_{SD}/dV_{SL} (intensity plot) as a function of V_{SL} and V_{SR} for the same sample. $B = 1\text{ T}$ was applied to suppress superconductivity at $T = 50\text{ mK}$.

of maximum sensitivity. We show four periods of a sawtooth waveform, characteristic of single electron transfer between the two dots (inset Fig. 2) [17]. The sawtooth can be understood as a steady polarization of the system until it becomes energetically favourable for an electron to be transferred. The polarization and charging behaviour then repeats quasi-periodically. The transfer events occur with an average period of $V_{SL}=24\text{ mV}$ over a wide range of gate voltages. We note that these events are not perfectly periodic and additional charge noise is also present, discussed below.

To more clearly resolve the electron transfer events, in Fig. 2b we map the data in 2D voltage space by plotting (dI_{SD}/dV_{SL}) as a function of the two gate voltages V_{SL} and V_{SR} . The locus of the charge transfer events is highlighted by the dark lines, indicating high transconductance. These follow linear trajectories and show a period of 24 mV in V_{SL} and 224 mV in V_{SR} , indicating a stronger capacitive coupling of the DQD to the left symmetry gate S_L than to S_R . This can be explained by lithographic alignment errors between the surface gates and the buried DQD. We have measured five DQD devices, with dot separations of $d=80\text{ nm}$, 100 nm and three with 150 nm . All show the characteristic quasi-periodic sawtooth seen in Fig. 2, but in each case the relative coupling capacitance and period varies due to differing misalignment. We have calculated the capacitance matrix for our devices for varying displacement between the surface gates and buried DQDs, finding values consistent with our data [18]. Displacements of order 50 nm can modify the capacitance or transfer period by up to an order of magnitude. Such misalignments lead to the B gate not being well centred between the dots, making

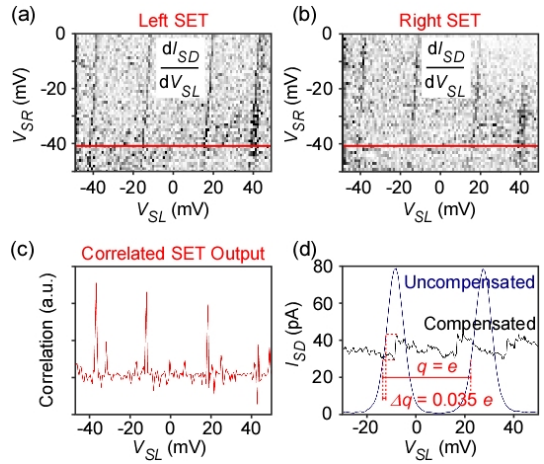


FIG. 3: Electron transfer events observed in dI_{SD}/dV_{SL} of **a**) left SET, and **b**) right SET, as a function of V_{SL} and V_{SR} for a DQD sample with $d=100\text{ nm}$. **c)** Correlated SET output plotted against V_{SL} (red line in **a,b**). Sharp peaks correspond to single electron transfer events. **d)** Determination of induced charge Δq due to a single electron transfer event within the DQD sample. The blue trace is the (uncompensated) SET current exhibiting characteristic Coulomb oscillations in V_{SL} . For the inter-dot transfer event we deduce $\Delta q = 0.035e$. $T = 50\text{ mK}$, $B = 1\text{ T}$.

control of the barrier between the QDs difficult. Improvements in lithographic alignment procedures will address this issue in future devices.

Whilst in principle a single SET is sufficient to detect charge transfer within the DQD (or Si:P qubit), by correlating the output from two SETs [17] it is possible to reject spurious events resulting from charge motion in the substrate, or within the SETs themselves. Figs. 3a,b show simultaneous measurement of both SETs on the DQD with $d=100\text{ nm}$, taken after thermal cycling to room temperature. Correlated detection now provides strong evidence that the charge transfer is occurring *in the region between* the two SET couplers. A simple correlation achieved by multiplying the two transconductance signals for the right and left SETs is shown in Fig. 3c for $V_{RC} = -41\text{ mV}$. The correlation signal exhibits a sharp peak whenever a charge transfer event occurs, whilst uncorrelated events are suppressed. The magnitude of the charge signal Δq induced on a SET island due to the electron transfer is a key parameter characterizing the time required for the readout process. We find $\Delta q = 0.035e$ for a DQD with $d=100\text{ nm}$ (Fig. 3d) and $\Delta q = 0.038e$ for a $d=150\text{ nm}$ sample, consistent with values obtained from a simplified model of our structure and similar to that obtained for a SET coupled to a Cooper pair box qubit by Duty et al. [19] ($\Delta q = 0.04e$).

Readout of qubits requires detectors that operate on time scales faster than the qubit relaxation (or excitation) time. Towards this goal the radio-frequency SET [20](rf-SET) is a promising candidate, combining near quantum-limited sensitivity [20, 21] with switchable back-action [22]. Large (100 MHz) measurement band-

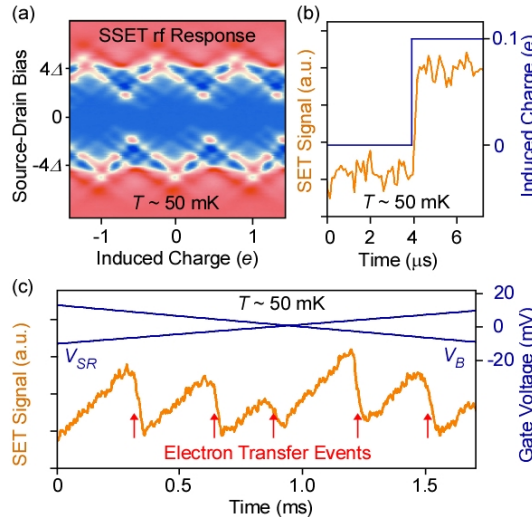


FIG. 4: Measurements using rf-SET detection. **a)** Bias spectroscopy of a rf-SET in the superconducting state ($B = 0T$) where Δ is the superconducting gap for Al. **b)** Single-shot response of the rf-SET to a small step in gate voltage creating an induced charge of $0.1e$ at the SET island. **c)** Characteristic sawtooth signature of periodic electron transfer in a DQD with $d = 150\text{nm}$, observed in the rf-SET signal (left axis scale) as a function of time while a differential bias voltage (right axis scale) is applied to control gates B and S_R . Data is an average of 16 traces, each with acquisition time 1.7 ms.

widths can be achieved by embedding the SET detector in a LC matching network, mapping dc conductance to reflected rf power. In rf measurements with $B = 0T$, the SET source-drain bias data (Fig. 4a) exhibit a typical Josephson quasiparticle spectrum. To maximize the detection signal we bias the SET to a region of small differential resistance ($V_{SD} \simeq 4\Delta$), where the sensitivity exceeds $10^{-5}e/\sqrt{\text{Hz}}$ as we have demonstrated [23]. Fig. 4b shows the time-domain response of an rf-SET to a step impulse applied to a SET bias gate. The gate signal induces a charge of $\Delta q = 0.1e$ on the SET island. Fig. 4c shows the output signal from one rf-SET on a DQD device with $d = 150\text{nm}$ as a function of time while a differential bias is applied between the control gates V_B and V_{SR} . Here again, the rf signal shows a characteristic sawtooth response, indicating periodic transfer of single electrons between the buried phosphorus dots. The quality of the rf response is greater than the dc data in Fig. 2a because it is possible to perform signal averaging on short timescales.

A number of control experiments were also carried out on the DQDs and related devices. The integrity of the ion-stopping mask was confirmed by fabricating nanocircuitry as in Fig. 1a but omitting the apertures for substrate doping. These devices showed no evidence of pe-

riodic charge motion in the substrate. To test the effectiveness of the anneal we measured electrical transport in Si:P nanowires (depth 20nm, width 50nm, length 1.8 μm) fabricated using an identical 14 keV P^+ implant, which confirmed that the P dopants were activated. The metallic density of states in the dots was confirmed by the observation of 75 electron transfers in the voltage range $V_{SL} = [-900\text{mV}, 900\text{mV}]$, all with a period close to 24 mV and all with the same slope in gate bias (Fig. 2a, 3a,b). Small variations in periodicity, seen in all data, are believed to be related to internal physical and electronic structure of the dots. Control devices with no implants, or with silicon implants, but with the same SET and gate structures were measured under identical conditions. No periodic transfer was seen in these although random charge transfer features, most likely due to electron traps in the substrate, were observed [24]. Devices configured with just a few P atoms also showed only a few electron transfer events as expected.

The results here demonstrate a new gate-controlled quantum dot system with the facility for fast measurement of inter-dot electron transport. To our knowledge these Si:P QDs are the only type defined by localized doping of silicon and may be applied to many proposed QD applications, e.g., quantum dot cellular automata [25], [26] networks. They can also be reduced to single atom dots using single-ion implantation [27, 28]. Our scheme [27] (Fig. 1b) uses in-situ ion detector electrodes to produce a signal each time a single P^+ ion enters the device, allowing ion counting.

Most importantly, the quantum dot devices demonstrated here represent a critical step towards silicon-based quantum computing, being configured with control and readout circuitry at the scale required for a two-atom Si:P charge qubit. The fast detection of single electron transfer over a distance of order 100nm provides good prospects for qubit readout, while correlated twin-SET detection offers additional immunity from materials-related charge noise. Future experiments will involve new buried architectures, combining precise dopant placement using scanned-probe lithography [29, 30] with surface SET readout, together with microwave spectroscopy on both DQD and two-P-atom devices to map out the energy levels and determine T_1 and T_2^* .

This work was supported in part by the Australian Research Council, the Australian Government, the U.S. National Security Agency, the Advanced Research and Development Agency and the U.S. Army Research Office under contract no. DAAD19-01-1-0653. We acknowledge E. Gauja, R. Starrett and A. Greentree for useful discussions.

[1] For a general review see: M. A. Nielsen and I. L. Chuang, *Quantum Computation and quantum information*, Cambridge University Press, (2000).

[2] Y. Nakamura, Yu A. Pashkin and J.S. Tsai, *Nature* **398**,

786 (1999).

[3] T. Yamamoto, Y. A. Pashkin, O. Astafiev, Y. Nakamura and J. S. Tsai, *Nature* **425**, 941 (2003).

[4] T. Hayashi, T. Fujisawa, H. D. Cheong, Y. H. Jeong and Y. Hirayama, *Phys. Rev. Lett.* **91**, 226804 (2003).

[5] J.M. Elzerman, R. Hanson, L.H. Williams van Beveren, B. Witkamp, L.M.K. Vandersypen and L.P. Kouwenhoven *Nature* **430**, 431 (2004).

[6] J.R. Petta, A.C. Johnson, C.M. Marcus, M.P. Hanson and A.C. Gossard, *Phys. Rev. Lett.* **93**, 186802 (2004).

[7] B. E. Kane, *Nature* **393**, 133 (1998).

[8] R. Vrijen, E. Yablonovitch, K. Wang, H.W. Jiang, A. Balandin, V. Roychowdhury, T. Mor and D. DiVincenzo, *Phys. Rev. A* **62**, 012306 (2000).

[9] M. Friesen, P. Rugheimer, D. E. Savage, M. G. Lagally, D. W. van der Weide, R. Joynt, and M. A. Eriksson, *Phys. Rev. B* **67**, 121301(R) (2003).

[10] R. de Sousa, J. D. Delgado, and S. Das Sarma, *Phys. Rev. A* **70**, 052304 (2004).

[11] C. D. Hill, L. C. L. Hollenberg, A. G. Fowler, C. J. Wellard, A. D. Greentree, and H.-S. Goan, *quant-ph/0411104*.

[12] L. C. L Hollenberg, A. S. Dzurak, C. Wellard, A. R. Hamilton, D. J. Reilly, G. J. Milburn and R. G. Clark, *Phys. Rev. B* **69**, 113301 (2004).

[13] D.N. Jamieson, C. Yang, T. Hopf, S.M. Hearne, C.I. Pakes, S. Prawer, M. Mitic, E. Gauja, S.E. Andresen, F.E. Hudson, A.S. Dzurak, R.G. Clark, *Appl. Phys. Lett.*, **86** 202101 (2005).

[14] D.R. McCamey, M. Francis, J.C. McCallum, A.R. Hamilton, A.D. Greentree and R.G. Clark, *Semicond. Sci. Technol.* **20** 363 (2005).

[15] P. M. Fahey, P. B. Griffin and J. D. Plummer, *Rev. Mod. Phys.* **61**, 289 (1989).

[16] T. A. Fulton and G. J. Dolan, *Phys. Rev. Lett.* **59**, 109 (1987).

[17] T. M. Buehler, D. J. Reilly, R. Brenner, A. R. Hamilton, A. S. Dzurak and R. G. Clark, *Appl. Phys. Lett.* **82**, 577 (2003).

[18] K. H. Lee, A. D. Greentree, J. P. Dinale, C. C. Escott, A. S. Dzurak and R. G. Clark, *Nanotechnology* **16** 74 (2005).

[19] T. Duty, D. Gunnarsson, K. Bladh and P. Delsing, *Phys. Rev. B* **69**, 140503 (2004).

[20] R. J. Schoelkopf, P. Wahlgren, A. A. Kozhevnikov, P. Delsing and D. E. Prober, *Science* **280**, 1238 (1998).

[21] A. N. Korotkov, *Phys. Rev. B* **49**, 10381 (1994).

[22] G. Johansson, A. Käck and G. Wendin, *Phys. Rev. Lett.* **88**, 046802 (2002).

[23] T. M. Buehler, D. J. Reilly, R. P. Starrett, N. A. Court, A. R. Hamilton, A. S. Dzurak and R. G. Clark, *J. Appl. Phys.* **96** 4508 (2004).

[24] M. Furlan and S. V. Lotkhov, *Phys. Rev. B* **67**, 205313 (2003).

[25] P. D. Tougaw and C. S. Lent, *J. Appl. Phys.* **75**, 1818 (1994).

[26] J. H. Cole, A. D. Greentree, C. J. Wellard, L. C. L. Hollenberg, and S. Prawer, *Phys. Rev. B* **71**, 115302 (2005).

[27] R. P. McKinnon, F. E. Stanley, N. E. Lumpkin, E. Gauja, L. D. Macks, M. Mitic, V. Chan, K. Peceros, T. M. Buehler, A. S. Dzurak, R. G. Clark, C. Yang, D. N. Jamieson and S. Prawer, *Smart. Mater. Struct.* **11**, 735 (2002).

[28] T. Schenkel, A. Persaud, S. J. Park, J. Nilsson, J. Bokor, J. A. Liddle, R. Keller, D. H. Schneider, D. W. Cheng and D. E. Humphries, *J. Appl. Phys* **94**, 7017 (2003).

[29] S. R. Schofield, N. J. Curson, M. Y. Simmons, F. J. Ruess, T. Hallam, L. Oberbeck and R. G. Clark, *Phys. Rev. Lett.* **91**, 136104 (2003).

[30] J. R. Tucker and T. -C. Shen, *Sol. Stat. Electr.* **42**, 1061 (1998).